Chiang Mai J. Sci. 2012; 39(4) : 623-638
http://it.science.cmu.ac.th/ejournal/
Contributed Paper

Evaluation of Precipitation Simulations over Thailand using a WRF Regional Climate Model

Chakrit Chotamonsak*[a], Eric P. Salathé Jr. [b], Jiemjai Kreasuwan [c] and Somporn Chantara [d]

[a] Environmental Science Program and Centre for Environmental Health, Toxicology and Management of Chemicals (ETM)., Faculty of Science, Chiang Mai University, Chiang Mai 50200, Thailand .

[b] Science and Technology Program, University of Washington, Bothell, Washington, USA.

[c] Department of Physics and Materials Science, Faculty of Science, Chiang Mai University, Chiang Mai 50200, Thailand.

[d] Environmental Science Program and Department of Chemistry, Faculty of Science, Chiang Mai University, Chiang Mai 50200,Thailand.

*Author for correspondence; e-mail: chotamonsak@gmail.com

Received: 24 August 2011
Accepted: 5 February 2012

ABSTRACT

The Weather Research and Forecasting (WRF) model is widely used as a regional climate model for dynamical downscaling in many regions world-wide. This study evaluates the WRF model for regional climate applications over Thailand, focusing on simulated precipitation using various convective parameterization schemes available in WRF. The NCEP/NCAR Reanalysis are used as forcing boundary data. The WRF simulations were performed at a 20-km grid spacing with an outer 60-km nest, to which the boundary forcing was applied. Experiments are presented for the year 2005 using four convective cumulus parameterization schemes, namely, BMJ (Betts-Miller-Janjic), GD (Grell-Devenyi), G3D (improved Grell-Denenyi) and KF (Kain-Fritsch) with and without nudging applied to the outermost nest. Results are evaluated both against station data and gridded observations. In general, the experiments with nudging perform better than un-nudged experiments and the BMJ cumulus scheme with nudging yields the smallest bias relative to observations.

Keywords: WRF, Regional climate model, dynamical downscaling, model evaluation, convective parameterization, precipitation, Thailand

1. INTRODUCTION

A sensitivity study of atmospheric model simulations to various cumulus parameterization schemes is an important topic not only in numerical weather prediction [1-3] but also in climate modeling studies [4-8]. Previous studies have confirmed that none of the available cumulus schemes is able to produce a perfect simulation of precipitation in their model domains. Wang and Seaman [2] compared precipitation results from four cumulus parameterization schemes in MM5 model, namely, the Anthes-Kuo, Betts-Miller, Grell, and Kain-Fritsch schemes. They found that the 6-h precipitation forecast skill for these schemes was fairly good, even for higher precipitation

thresholds. They also found that the forecast skill was generally higher for cold-season events than for warm-season events, and the model's precipitation forecast skill was better in rainfall volume than in either the areal coverage or the peak amount. Furthermore, they found that the Kain-Fritsch method appeared to perform better compared to other parameterizations. However, this does not necessarily mean that the Kain-Fritsch scheme is superior for other regions, seasons, or combinations with other physical processes in the model. For example, the Betts-Miller scheme available in the MM5 model has shown the best performance for maximum rainfall forecasts over the Taiwan area [9] while the Grell cumulus convection scheme has been found to perform best in a Bay of Bengal tropical cyclone study [10]. In another study, Lee at al. [7] found that the Anthes-Kuo scheme reproduced the East Asian Summer precipitation properly while the Grell scheme was on the whole suitable to simulate the general features of East Asian summer monsoon for four months (MJJA) simulation in 1998. Pattanaik et al. [11] compared the sensitivity of three cumulus parameterization scheme in WRF model in forecasting the monsoon depression over India. They found that the overall rainfall forecast associated with the monsoon depression was captured well in WRF model with KF scheme compared to that of GD scheme and BMJ scheme with observed heavy rainfall. While Mukhopadhyay et al [12] shown that the Betts-Miller-Janjic (BMJ) cumulus scheme was found to produce better results compared to other cumulus schemes over the same region. Therefore, the evaluation of precipitation and other variables produced by alternative cumulus parameterization schemes and others physics process available in models, is an important step in developing climate simulations over selected regions.

When using coarse-scale data (either from a reanalysis or a GCM) as lateral boundary conditions driving a regional climate model without any further nudging, the interior meteorological fields simulated by the regional model can deviate significantly from those of the driving fields [13]. Four-dimensional data assimilation (FDDA) techniques provide one way to constrain the RCM and keep it from diverging too far from the coarse-scale fields. The understanding of the influence of nudging for regional climate modeling has become an interested area of research. There has been comparatively limited effort to understand the effects of nudging using the regional climate models. For example, Bowden et al. [13] used WRF model to evaluate interior nudging techniques using the Weather Research and Forecasting (WRF) model for regional climate modeling over the contiguous United States (CONUS) by nudging only at the lateral boundaries, using grid point (i.e. analysis) nudging, and using spectral nudging. They found that using interior nudging reduces the mean biases for 2-m temperature, precipitation, 500-hPa geopotential height, and 850-hPa meridional wind throughout the CONUS compared to the simulation without interior nudging. They also found that the predictions of 2-m temperature and fields aloft behave similarly when either analysis or spectral nudging is used. For precipitation, however, analysis nudging generates monthly precipitation totals, intensity and frequency of precipitation that are closer to observed fields than spectral nudging. Others study, Lo et al. [14] used WRF regional climate application to compare lateral boundary nudging, frequent re-initialization, and analysis nudging in the one-year simulations. They found that both analysis nudging and frequent re-initialization are effective to

constrain the large-scale circulation and improve the accuracy of the downscaled fields.

In this study, we provide additional insights into the advantages of using analysis nudging for continuous integrations in the WRF regional climate modeling applications. While WRF provides an option for spectral nudging, experiments were performed only using analysis nudging, following the methods of Mass et al [26] where nudging is applied only to the outer domain, with the inner domain forced only at the boundaries. This approach achieves one of the benefits of spectral nudging, which is to constrain only the large-scale patterns in the simulation. However, this study does not comprehensively address all aspects of using nudging in WRF for regional climate modeling, which would include variations in the nudging parameters, the use of spectral nudging, and other approaches to nudging across model nests.

The objective of this study is to evaluate the precipitation results in eight WRF regional climate simulations with a two-nest model configuration over Thailand using reanalysis boundary conditions for the year 2005. We compare four different cumulus parameterization schemes with and without analysis nudging applied to the outer domain. Our analysis focuses in particular on reproduction of the observed precipitation.

This study is focused over Thailand, which is a region characterized by several seasonal and climatic features with complex terrain and coastlines. Thailand lies within the humid tropics and remains warm throughout the year. Annual mean temperatures vary from the north to the south, with different regional rainfall regimes prevailing in dry northeast and wet southwest. With the exception of the southern isthmus, which receives rainfall throughout the year, Thailand has a dry season that extends from November to April corresponding with the period of the Northeast monsoon, marked by cool-dry (November to February) and hot-dry (March and April) periods. A hot-wet rainy season prevails from May to October, corresponding with the Southwest monsoon. Thailand has wide variations in extremes of temperature at different locations. The coastal area along the Andaman sea (west coast) and China sea (east coast) (as shown in Figure 1) is usually

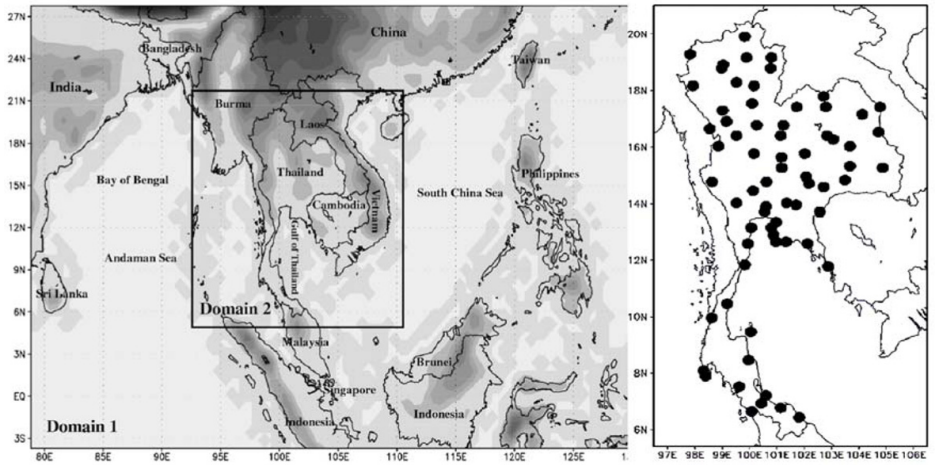

Figure 1. Model domains (left) and station locations used for model evaluation (right). The outer domain is 60 km and the nested domain is 20 km horizontal resolution, respectively. The shading indicates topography.

warm throughout the year, whereas the mountainous area far north is relatively cool in winter.

2. EXPERIMENTAL DESIGN

2.1 Regional Climate Model and Forcing Data

The model used in this study is the Weather Research and Forecasting (WRF) model, developed at the National Center for Atmospheric Research (NCAR). WRF is an advanced mesoscale numerical weather prediction system designed to serve both operational forecasting and atmospheric research needs (http://www.wrf-model.org). The model configuration used here follows that of the WRF regional climate model used in previous studies [15, 16]. The fixed physics options used in this study include the WRF Single-Moment 6-Class Microphysics (WSM6) scheme [17], Dudhia shortwave radiation [18] and Rapid Radiative Transfer Model (RRTM) long-wave radiation [19], the Yonsei University planetary boundary layer (PBL) scheme [20] , and the Noah Land Surface Model (LSM) 4-layer soil temperature and moisture model with canopy moisture and snow-cover prediction [21]. The four different cumulus parameterization schemes used in this study are those available in WRF ARW vision 3.1: Betts-Miller-Janjic (BMJ) [22], Grell-Devenyi ensemble scheme (GD) [23], Grell 3d ensemble cumulus scheme (G3D), and Kain-Fritsh scheme (KF) [24]. The 2.5x2.5 degree NCEP/NCAR Reanalysis [25] were used as the forcing data to provide initial and boundary conditions. The boundary conditions were updated 6 hourly. We use NCEP/NCAR reanalysis data to satisfy a prerequisite for estimating climate change projections by assessing the ability of the model to simulate current climate and its physical processes. The WRF regional climate model was run using one-way nesting at 60-km and 20-km horizontal grid spacings and 28 vertical levels with 10 mb of the top model. The inner domain, with a 20-km grid spacing covering Thailand and neighboring countries, was analyzed in this study, Eight simulations were performed with and without nudging applied for all four cumulus schemes. Nudging with Newtonian relaxation (grid or analysis nudging) on the driving fields for wind, temperature and moisture was applied at all vertical levels in the 60-km WRF outer domain in order to keep the simulated states close to the large-scale states of the reanalysis fields. Nudging was not applied to the inner 20-km domain, which allowed the WRF model to generate small-scale features. This approach addresses the dual objectives of downscaling, which is to generate mesoscale meteorological details while maintaining consistency with the large-scale state [26, 27]. The nudging terms used in these experiments are taken from Mass et al [26] ($u=0.0001$, $v=0.0001$, $t=0.0001$, $q=0.000001$). The equations and further details of analysis nudging can be found in Stauffer and Seaman [28] and Stauffer et al. [29]. The WRF runs were initialized at 0000 UTC 1 December, 2004 and ended at 0000 UTC 1 January, 2006 for a one-year (2005) simulation. The first month simulation (December 2004) was regarded as model spin-up and excluded from analysis. The model output was hourly. Table 1 summarizes the selected physics options and experimental design while Table 2 lists the simulation experiment names and design specifics.

2.2 Observational data

The observational data used for model evaluation in this study are measurements made at 69 stations of the Thai Meteorological Department (TMD), selected with more than 95% data available for the year 2005.

Table 1. Physics process and options used in this study.

Physics Process and options	Selected Option
Microphysics	WSM6
Cumulus parameterization	BMJ, GD, G3D and KF
Short-wave radiation	Dudhia
Long-wave radiation	RRTM
Planetary Boundary Layer (PBL)	Yonsei University
Grid analysis nudging	No nudging and nudging
SST update	6 hourly update
Run period	1 year (2005)

The location of stations is shown in Figure 1. Another data set used for spatial evaluation is the high-resolution (0.5×0.5 degree) gridded data over global land areas [30, 31] available through the Climatic Research Unit (CRU TS3.0, 2008) at the University of East Anglia.

3. RESULTS

Below we present results from the eight WRF simulations to evaluate the relative performance of the different convective parameterizations and the effect of nudging. Comparisons are made against both station observations and gridded precipitation.

3.1 Station Results

Figure 2 shows scatter plots of daily mean precipitation for all seasons between station observations and WRF simulations at all 69 stations. Each solid circle in Figure 2

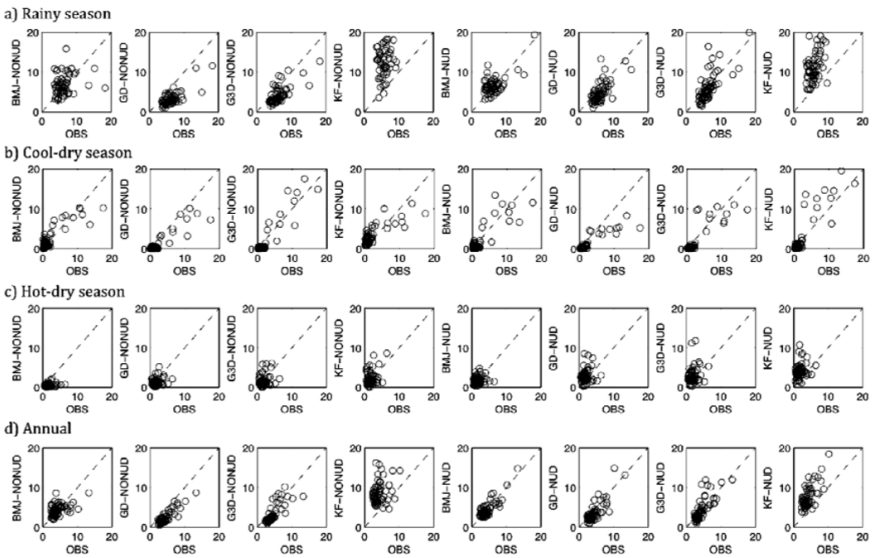

Figure 2. Scatter plots of daily mean precipitation between station observed and WRF simulated at 69 stations for rainy season (a), cool-dry season (b), hot-dry season (c) and annual (d) for BMJ-NONUD (1st column), GD-NONUD (2nd column), G3D-NONUD (3rd column), KF-NONUD (4thcolumn), BMJ-NUD (5th column), GD-NUD (6th column), G3D-NONUD (7th column) and KF-NONUD (8th column). Each scatter marker represents one station.

represents the daily mean precipitation at one station for the indicated season. Table 3 and Table 4 list the correlation coefficient, regression slope (from Figure 2), bias and absolute bias (average absolute difference between observed and simulated values) of precipitation between the 69 station observations and WRF simulations averaged over rainy, cool-dry, hot-dry season and annual mean, for the four no-nudge experiments (Table 3) and the four nudge experiments (Table 4). The statistical significance of the correlation coefficient was found using a Students t-test with 69 degrees of freedom (*i.e.* assuming stations are statistically independent). In Tables 3 and 4, correlation coefficients that are significant at 99% are indicated in bold; correlations are significant for all simulations except in the hot-dry season when none of the simulations produces statistically significant correlation with observations.

Table 3 and Table 4 indicates that, for the rainy season, nudging improves all simulations both for slope and absolute bias, indicating that the nudged simulations better represent both the observed range and magnitude of precipitation. Nudging consistently improves results for rainy-season precipitation for all parameterizations as indicated by absolute bias, relative bias, and slope. Results for correlation are comparable or better (BMJ, K-F) when nudging is employed. For the two dry seasons, nudging makes less difference in the results, with some

Table 3. The correlation coefficient, regression slope (from Figure 2) , biases and absolute bias of precipitation over all 69 stations between observation and WRF simulation for rainy, cool-dry and hot-dry season and annual using four different cumulus parameterization schemes with outermost domain no nudging applied. The blue color indicate the best score while the red color is the worst score. The correlation coefficients that are significant at 99% are indicated in bold (using Student t-test).

Time Scale	Statistic Score	BMJ-NONUD	GD-NONUD	G3D-NONUD	KF-NONUD
Rainy	Corr	**0.47**	**0.86**	**0.78**	**0.75**
	Slope	0.36	0.62	0.58	2.24
	Biases	0.33	-3.19	-2.27	8.94
	Abs bias	2.26	3.23	2.59	9.11
Cool-dry	Corr	**0.87**	**0.90**	**0.93**	**0.81**
	Slope	0.68	0.60	1.08	0.54
	Biases	0.04	-1.05	-0.39	0.84
	Abs bias	1.01	1.08	0.98	1.60
Hot-dry	Corr	0.15	0.21	0.25	0.28
	Slope	0.06	0.17	0.31	0.43
	Biases	-1.3	-0.63	-0.34	0.41
	Abs bias	1.31	1.06	1.13	1.25
Annual	Corr	***0.47***	***0.88***	***0.79***	***0.60***
	Slope	0.32	0.71	0.88	1.49
	Biases	0.08	-2.09	-1.37	4.99
	Abs bias	1.25	2.09	1.71	5.07

Table 4. As table 3 but the nudging experiments.

Time Scale	Statistic Score	BMJ-NUD	GD-NUD	G3D-NUD	KF-NUD
Rainy	Corr	**0.79**	**0.85**	**0.79**	**0.86**
	Slope	0.80	1.09	0.96	2.16
	Biases	0.26	-1.22	-0.40	6.18
	Abs bias	1.65	2.03	1.83	6.32
Cool-dry	Corr	**0.85**	**0.89**	**0.85**	**0.89**
	Slope	0.80	0.46	0.77	1.20
	Biases	-0.30	-1.09	-0.53	0.44
	Abs bias	1.11	1.12	1.05	1.12
Hot-dry	Corr	0.13	0.18	0.20	0.19
	Slope	0.11	0.25	0.36	0.30
	Biases	-0.08	0.90	1.08	2.32
	Abs bias	0.91	1.49	1.60	2.46
Annual	Corr	**0.83**	**0.82**	**0.77**	**0.81**
	Slope	0.84	1.00	1.05	1.79
	Biases	0.05	-0.83	-0.18	3.69
	Abs bias	0.92	1.26	1.23	2.73

parameterizations performing better and some worse. For the hot-dry season, the WRF results perform relatively poorly for all configurations, making comparative evaluation difficult. Among parameterizations, the BMJ scheme shows the smallest absolute and total bias, both for no-nudged and nudged cases. This scheme, however, exhibits the lowest correlation (0.47) and slope (0.47) when used without nudging; other simulations show higher correlations, ranging from 0.75 to 0.86. The use of nudging, however, yields a much better improvement in the correlation score for BMJ than for other parameterizations, and BMJ-NUD has doubled the correlation score of BMJ-NONUD which is comparable to those of the other nudged experiments.

For the cool-dry season, all simulations show relatively high correlation (>0.8). There are substantial differences among the simulations in regression slopes, with all simulations underestimating the observed range except for the KF-NUD (1.2) and G3D-NONUD (1.08) cases. The un-nudged BMJ simulation produces the smallest bias, with a slight increase in bias with nudging. Overall, however, nudging makes little difference in model scores for the experiments.

For the hot-dry season, all experiments show rather low correlations (< 0.29) and regressions slope (<0.44). Biases are large with the exception of BMJ, which shows substantial reduction in bias for the nudged case.

In general, we found that the KF parameterization, with or without nudging, consistently overestimated precipitation for all seasons with the lowest (highest) bias for the hot-dry (rainy) season. Nudging reduced the bias in all seasons except for the hot-dry. The GD and G3D parameterizations underestimate precipitation in all seasons, and the bias is reduced with nudging for the rainy and cool-dry seasons.

However, nudging results in a positive bias for the hot-dry season. The BMJ-NONUD shows slight overestimation in the rainy and cool-dry seasons but underestimation in the hot-dry season with an average bias of -1.3 mm/day. The BMJ method yields the smallest bias compared to other simulations (except for the un-nudged hot-dry case) and the use of nudging generally reduces the bias except in the cool dry season when nudging introduces a small dry bias.

The temporal correlation coefficients of simulated and observed daily precipitation at all 69 stations in Thailand show mostly low correlation (not shown). High correlation of daily precipitation requires the simulation to accurately represent the timing of convective precipitation events to within a 24-hour period, which is a demanding test given the coarse (2.5×2.5 degree) forcing data. To examine the correlation over longer time scales, which are better resolved by the reanalysis, the 5-day and 30-day timescales are examined following Zhang *et al*. [16]. The running means of the observed and WRF simulated precipitation time series at each station was calculated and the correlation coefficients was calculated at corresponding stations. Figure 3 shows the 5-day and 30-day run mean temporal correlation coefficients at all locations across Thailand. The number on the lower right corner of each plot indicates the averaged correlation over all stations. As in Zhang et al. [16], the correlation coefficients of all experiments have increased when averaging precipitation over increasing number of days. At 30-day averaging, the correlation is larger than 0.60 and essentially indicates that the simulation captures the annual cycle well.

3.2 Heavy and light precipitation

For climate studies, the probability of precipitation extremes, both dry days and heavy precipitation, is more important than the timing of events, which is reflected in the temporal correlations discussed above. To compare the simulated precipitation intensities with the observations, Figure 4 shows the histogram of daily precipitation from all 69 stations. We find that the BMJ scheme reproduces the frequency of precipitation at all thresholds, with or without nudging. The GD and G3D schemes over-predict light precipitation (<10 mm/day), reproduce moderate precipitation (10-20 mm/day) when nudging is applied, and under estimate heavy precipitation. KF under-predicts light precipitation, represents moderate precipitation well, and over-predicts heavy precipitation. The use of nudging generally improves the precipita-tion intensities for all schemes except for KF.

3.3 Spatial Patterns

To examine the spatial patterns, we shall now compare the simulated precipitation with the gridded CRU observations. The gridded CRU precipitation shows rather high correlation to station observations (Figure 5a) and low biases (Figure 5b). Thus, the results at station locations are similar using either the CRU or the station data. The typical seasonal precipitation distribution is shown in the CRU observations (Figure 5c). During the rainy season, heavy precipitation is found mainly along coastal areas, particularly the west coast of Thailand and Myanmar, with relatively drier conditions over the lowlands of the interior of Thailand. In the cool-dry season, heavy precipitation is observed only along the southern coast and the Malay peninsula. In the hot-dry season, the entire region is arid. This seasonal cycle reflects the onset

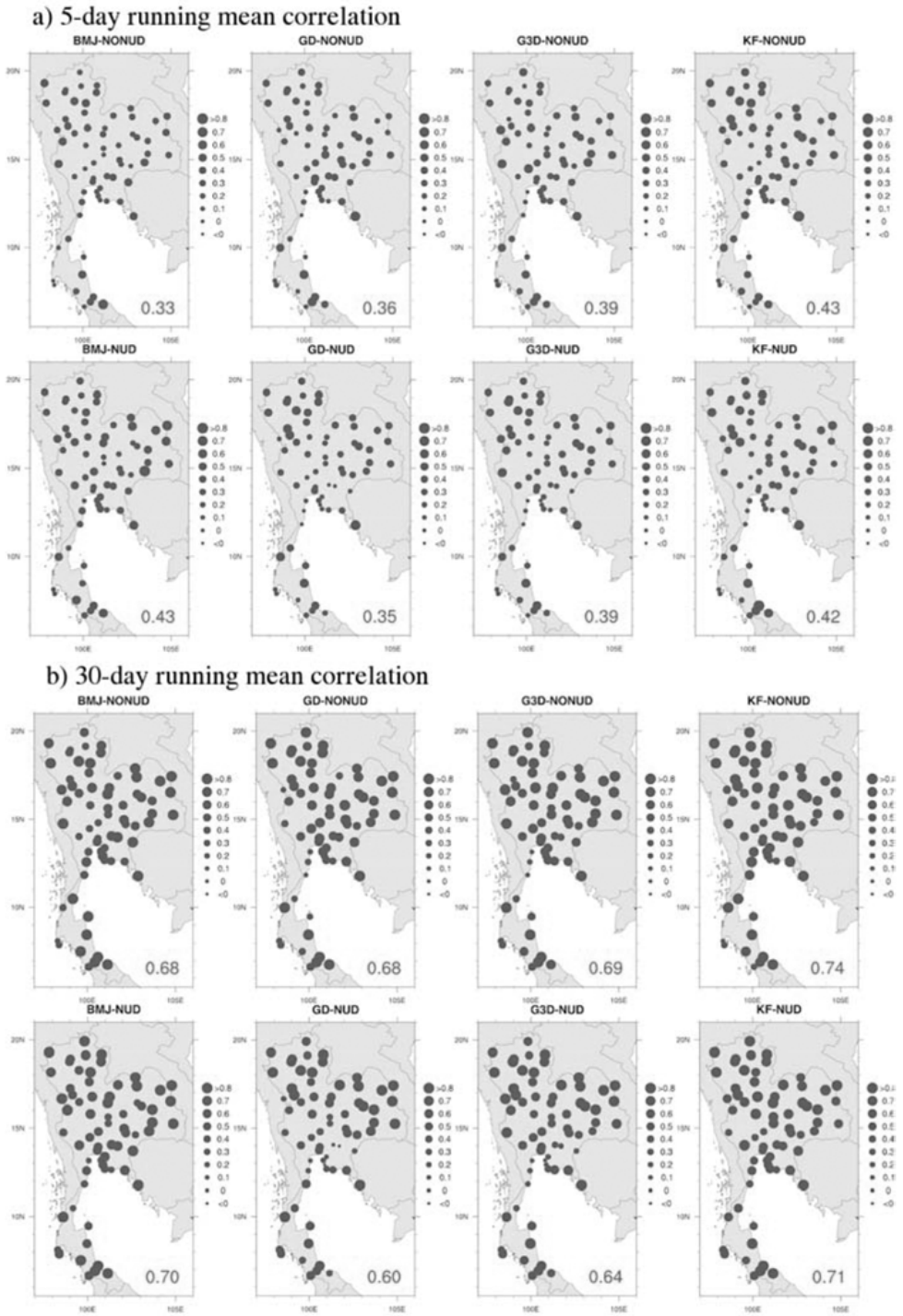

Figure 3. Temporal correlation of 5-day running mean (a) and 30-day running mean (b) of precipitation for all 69 stations between observation and WRF simulation for BMJ-NONUD (a), GD-NONUD (b), G3D-NONUD (c), KF-NONUD (d), BMJ-NUD (e), GD-NUD (f), G3D -NUD (g) and KF-NUD (h). The number on lower-right corner of each plot is the averaged correlation over 69 stations.

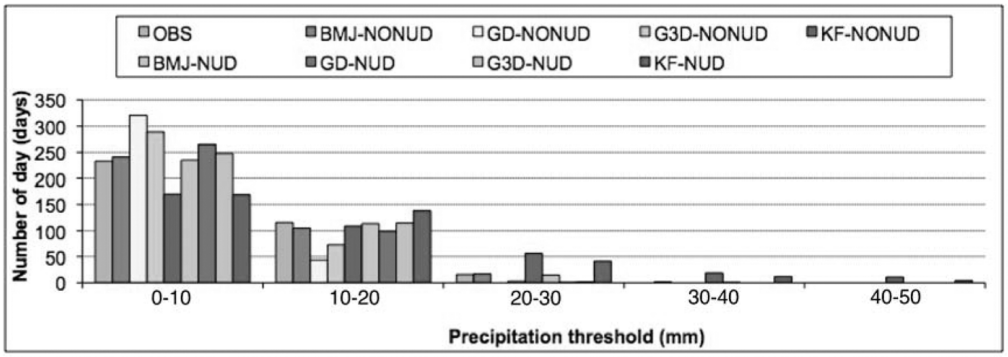

Figure 4. Histograms of daily of precipitation averaged over all 69 stations.

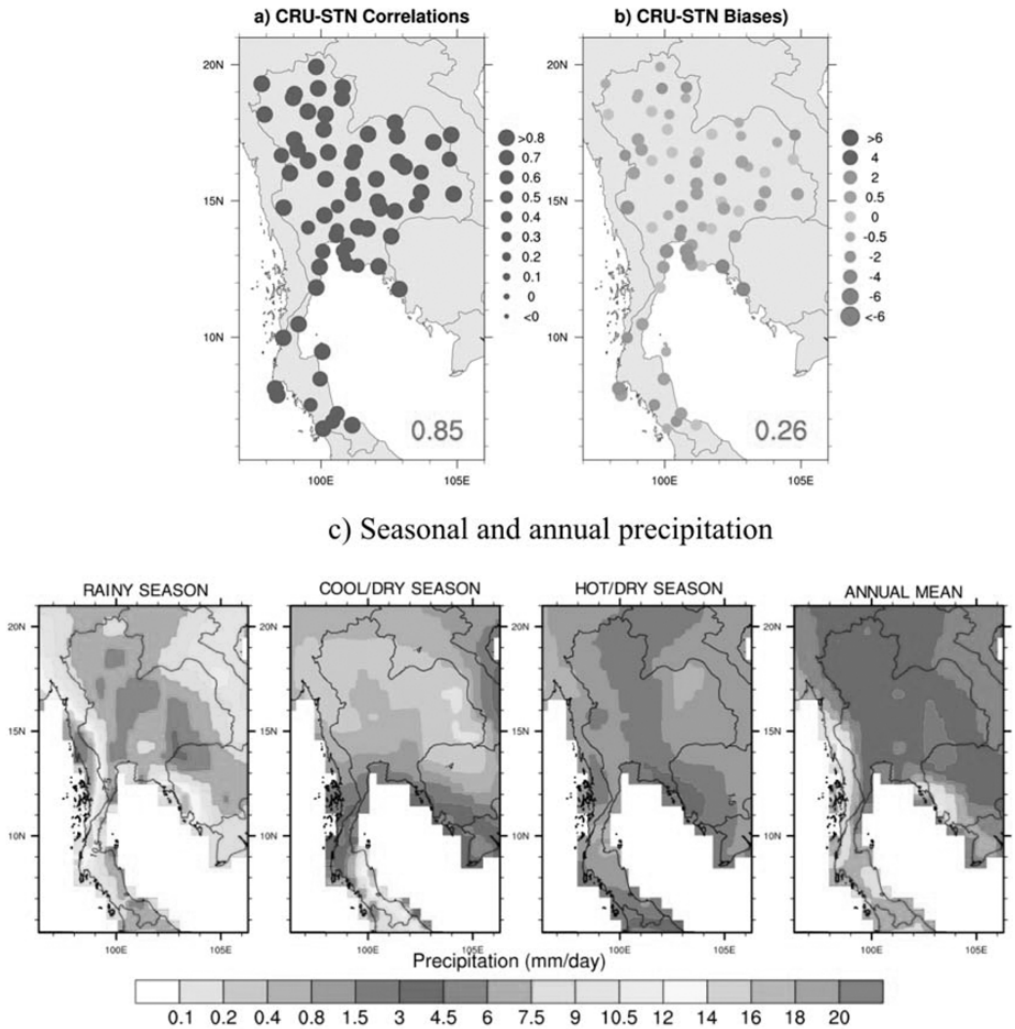

Figure 5. Correlation (a) and biases (mm/day) (b) of precipitation between the gridded CRU observations and station observations at 69 stations, and seasonal and annual mean CRU gridded precipitation (c). The numbers on the lower-right corners of (a) and (b) are the averaged value over 69 stations.

of south-westerly winds associated with the south-Asian monsoon and the cyclone season, the primary mechanisms for heavy precipitation over the region.

Figure 6 shows the bias between the WRF and CRU precipitation. We find substantial differences among simulations for the rainy season (1st row). The BMJ-NONUD simulation produces a slight dry bias in southern Thailand but wet bias in northern Thailand. Both these deficiencies are improved in the BMJ-NUD case. The GD and G3D simulations mostly under-predict precipitation over Thailand, with substantial improvement with nudging applied. The KF simulated precipitation is too high throughout Thailand and neighboring countries with only modest improvement from nudging. A consistent feature of most simulations (GD-NUD, G3D-NUD KF-NONUD and KF-NUD) is a relatively high wet bias in the rainy season along the Thanon Thongchai and Tanao Sri mountain ranges that form the Thailand-Burma border. Additionally, a wet bias is also noted along the mountainous southwestern coast of Cambodia in all experiments. In the GC-NUD and G3D-NUD experiments, there is also a dry bias on the opposite slopes of these mountains. During the south-west monsoon, these mountains form an orographic barrier, with heavy precipitation along the western and southern (*i.e.* windward) sides (see observations, Figure 5c) and rain shadowing on the opposite slopes. Despite overall improvement in the simulation with nudging, the nudged experiments tend to exaggerate this feature, with the BMJ-NUD showing distinctly better performance.

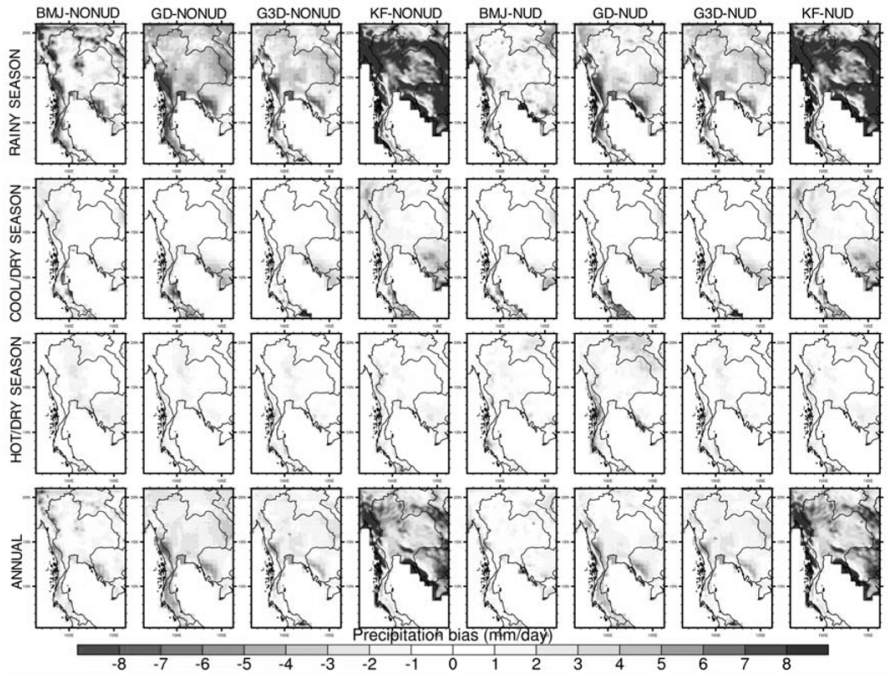

Figure 6. Seasonal mean precipitation bias (mm/day) between model simulated and observed for rainy (1st row), cool dry season (2nd row), hot dry season (3rd row) and annual mean (4th row) for BMJ-NONUD (1st column), GD-NONUD (2nd column), G3D-NONUD (3rd column), KF-NONUD (4th column), BMJ-NUD (5th column), GD-NUD (6th column), G3D -NUD (7th column) and KF-NUD (8th column).

The cool-dry season (Figure 6 2nd row) is characterized by dry conditions over the Northern, Central and Northeastern Thailand and heavy precipitation over southern Thailand. Other than BMJ-NONUD and KD-NONUD, all experiments produce similar precipitation patterns to the observed over the northern part, but vary over the south. The GD simulations show a dry bias over the entire south. The other simulations consistently produce too little precipitation along the southern coast and too much precipitation over the southern Malay Peninsula. This pattern suggests a general southward displacement of intense convection by the regional simulations, and may also result in part from deficiencies in the large-scale forcing.

Precipitation is infrequent during the hot-dry season (Figure 6 3nd row) and is mostly associated with scattered thunderstorms throughout the region. The experiments without nudging show small wet or dry biases depending on the location. With nudging, all parameterizations over-estimate precipitation, with the smallest bias noted for the BMJ scheme.

In the annual mean (Figure 6 4nd row), precipitation bias is dominated by that in the rainy season, but in many cases, seasonal biases cancel out each other resulting in better performance in reproducing the annual total rainfall. For the annual mean results, there is a clear improvement for simulations using nudging and for the BMJ parameterization.

3.4 The southwest monsoon

The monsoon, a system of winds that influences the climate of large area and that reverses direction with the seasons. Monsoons are caused primarily by the much greater annual variation in temperature over large areas of land than over large areas of adjacent ocean water. This variation causes an excess of atmospheric pressure over the continents in the winter, and a deficit in the summer. The disparity causes strong winds to blow between the ocean and the land, bringing heavy seasonal rainfall. In southeast Asia, a wind that is part of such a system and that blows from the southwest in the summer and usually brings heavy rain. Figure 7 shows the seasonal averaged wind direction simulated by WRF model using four different cumulus parameterization schemes with nudging for June-July-August, a typically strong southwest monsoon season. It was found that all cumulus parameterization schemes can capture the southwest monsoon well, compared to NCEP/NCAR reanalysis data. Also, Figure 8 shown daily averaged wind direction simulated from WRF model compared to observation and NCEP/NCAR reanalysis at Ubon Ratchathani (Figure 8.a) and Songkhla (Figure 8.b) stations, to show how well the WRF model capture the monsoon onset (wind reversal). Two stations are selected to show the daily surface directions avoid the topography affect. It was found that all schemes can capture the temporal of the monsoon onset (wind reversal) well compare to both the observation and reanalysis data.

4. CONCLUSIONS

In this paper, we have presented precipitation results from eight WRF regional climate model simulations covering a domain of southeast Asia centered over Thailand at 20-km resolution that is nested into a 60-km outer domain. The experiments simulated the year 2005 using large-scale forcing from the NCEP/NCAR reanalysis. The results

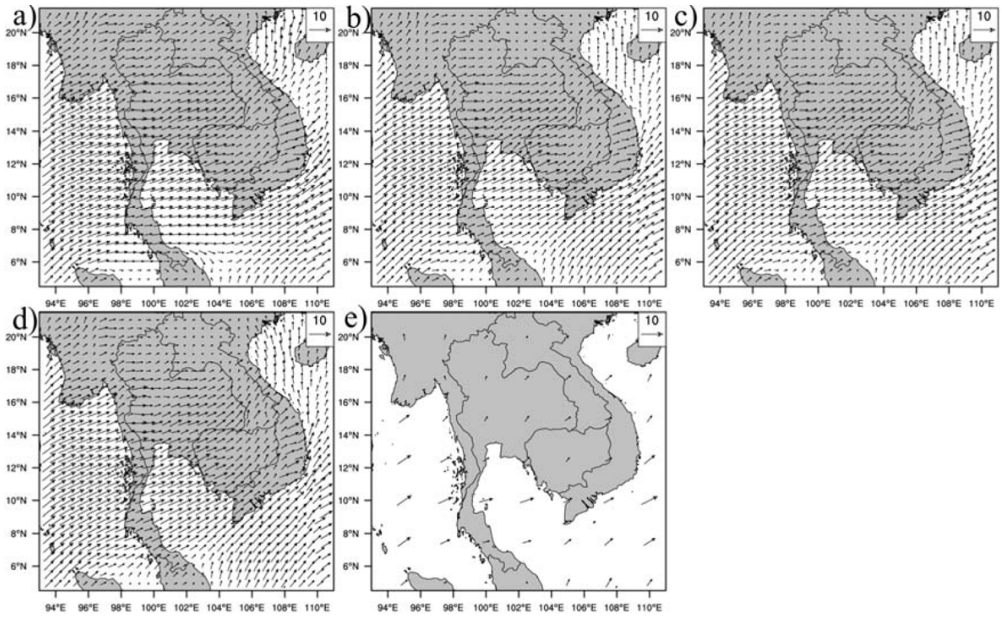

Figure 7. JJA mean surface wind simulated using a) BMJ scheme, b) GD scheme, c) G3D scheme and d) KF scheme compared to NCEP/NCAR reanalysis data.

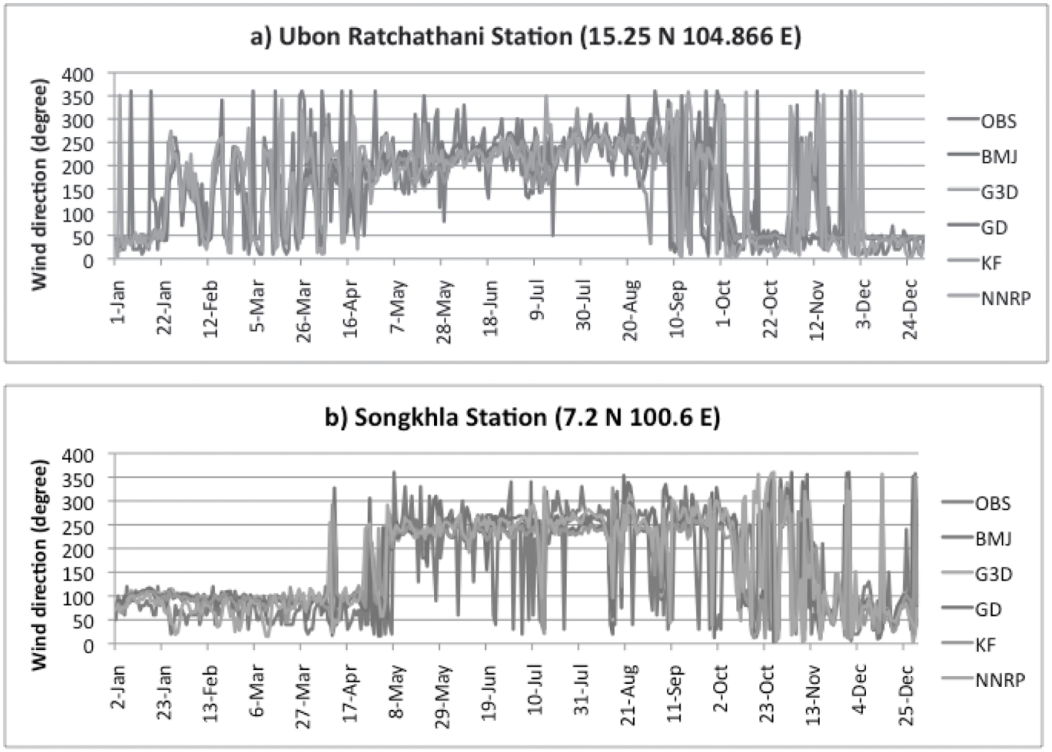

Figure 8. Daily mean surface wind direction at Ubon Rtachathani (a) and Songkla (b) station from WRF simulations using BMJ, GD, G3D and KF schemes, compared to station observed (OBS) and NCEP/NCAR reanalysis data (NNRP).

are evaluated against two observational datasets to establish both the overall skill of the regional model and its dependence on convective parameterization and the use of nudging. Four different convective parameterizations are used with and without nudging applied. In the nudged experiments, Newtonian relaxation is applied to the outmost (60-km) grid to maintain the large-scale structure of the forcing fields across the interior of the domain.

Our results show that differences in cumulus parameterizations and the application of nudging can have substantial impacts on simulated convection and precipitation. Deficiencies in simulated precipitation can result directly from the regional model, the convective parameterization used, or from the large-scale boundary conditions (*i.e.*, the reanalysis fields). It is difficult or impossible to isolate the sources of these errors since some errors may be related to deficiencies in internal model components or to the interactions and coupling of a cumulus parameterization scheme with other model components [2].

With these limitations in mind, the results presented here can give some guidance to configuring WRF for simulations over southeast Asia and the suitability of the model for regional climate simulations. There was no clear leader among the experiments that consistently performed better than the others. However, in general, nudging improved most simulations, especially in the rainy season. Overall, the BMJ scheme produced the smallest biases, both averaged over the domain and locally. In particular, BMJ produced the best probability distribution of precipitation, which is critical for climate simulations.

The WRF simulations show realistic monsoon flow over Thailand, and capture well the monsoon onset.

6. ACKNOWLEDGEMENTS

This research has been financially supported by the Science and Technology (S&T) Program, University of Washington Bothell for VISIT Program internship and Office of the Higher Education Commission , Ministry of Education, Thailand. The partially supported by the Graduate School, Faculty of Science, Chiang Mai University and Centre for Environmental Health, Toxicology and Management of Chemicals (ETM), Thailand. Global Reanalysis data from NCAR/NCEP, WRF model from NCAR and meteorological stations observed data from Thai Meteorological Department are highly appreciated. We also appreciate Rick Steed and Yongxin Zhang (now at NCAR) at University of Washington to provide model configure method and scripts. Dr. Cindy Bruyere at NCAR provided modified KF scheme (not included in this study) to compare with original KF scheme result are also appreciated. We also highly appreciate the Joint Institute for the Study of the Atmosphere an Ocean (JISAO), University of Washington as the constructive host and computer resource.

REFERENCES

[1] Kerkhoven E., Gan T.Y., Shiiba M., Reuter G. and Tanaka K., A comparison of cumulus parameterization schemes in a numerical weather prediction model for a monsoon rainfall event, *Hydrol. Process.*, 2006; **20:** 1961-1978.

[2] Wang W. and Seaman N.L., A comparison study of convective parameterization schemes in a mesoscale model, *Mon. Weathe.r Rev.*, 1997; **125:** 252-278.

[3] Ferretti R., Paolucci T., Zheng W., Visconti G. and Bonelli P., Analyses

of the precipitation pattern on the Alpine region using different cumulus convection parameterizations, *J. Appl. Meteorol.*, 2000; **39:** 182-200.

[4] Im E.S., Kim M.H., Kwon W.T. and Bae D.H., Sensitivity of recent and future regional climate simulations to two convection schemes in the RegCM3 nesting system, *J. Korean Meteor. Soc.*, 2007; **43:** 411-427.

[5] Giorgi F. and Shields C., Tests of precipitation parameterizations available in latest version of NCAR regional climate model (RegCM) over continental United States, *J. Geophy. Res-Atmos*, 1999; **104:** 6353-6375.

[6] Gochis D.J., Shuttleworth W.J.A. and Yang Z.L., Sensitivity of the modeled north American monsoon regional climate to convective parameterization, *Mon. Weather. Rev.*, 2002; **130:** 1282-1298.

[7] Lee D.K., Cha D.H. and Choi S.J.. A sensitivity study of regional climate simulation to convective parameterization schemes for 1998 east Asian summer monsoon, *Terr. Atmos. Ocean. Sci.*, 2005; **16:** 989-1015.

[8] Leung L.R., Zhong S.Y., Qian Y. and Liu Y.M., Evaluation of regional climate simulations of the 1998 and 1999 East Asian summer monsoon using the GAME/HUBEX observational data, *J. Meteorol. Soc. Jpn.*, 2004; **82:** 1695-1713.

[9] Yang M.J. and Tung Q.C., Evaluation of rainfall forecasts over Taiwan by four cumulus parameterization schemes, *J. Meteorol. Soc. Jpn.*, 2003; **81:** 1163-1183.

[10] Mandal M., Mohanty U.C. and Raman S., A study on the impact of parameterization of physical processes on prediction of tropical cyclones over the Bay of Bengal with NCAR/PSU mesoscale model, *Nat. Hazards.*, 2004; **31:** 391-414.

[11] Pattanaik D.R., Kumar A., Rao Y.V.R. and Mukhopadhyay B., Simulation of monsoon depression over India using high resolution WRF model - sensitivity to convective parameterization schemes, *Mausam*, 2011; **62(3):** 305-320.

[12] Mukhopadhyay P., Taraphdar S., Goswami B.N. and Krishnakumar K., Indian summer monsoon precipitation climatology in a high-resolution regional climate model: Impacts of convective parameterization on systematic biases, *Weather and Forecasting*, 2010; **25(2):** 369-387.

[13] Bowden J., Otte T., Nolte C. and Otte M., Examining interior grid nudging techniques using two-way nesting in the WRF model for regional climate modeling, *J. Climate*, 2011: doi:10.1175/JCLI-D-11-00167.1, in press.

[14] Lo J.C., Yang Z. and Pielke R.A., Assessment of three dynamical climate downscaling methods using the Weather Research and Forecasting (WRF) model, *J. Geophys. Res.*, 2008; **113:** D09112+, doi:10.1029/2007JD009216.

[15] Salathe E.P., Leung L.R., Qian Y. and Zhang YX., Regional climate model projections for the State of Washington, *Climatic Change.*, 2010; **102:** 51-75.

[16] Zhang Y.X, Duliere V., Mote P.W. and Salathe E.P., Evaluation of WRF and HadRM mesoscale climate simulations over the US Pacific northwest, *J. Climate*, 2009; **22:** 5511-5526.

[17] Hong S.Y., Dudhia J. and Chen S.H., A revised approach to ice microphysical

processes for the bulk parameterization of clouds and precipitation, *Mon. Weather, Rev.*, 2004; **132:** 103-120.

[18] Dudhia J., Numerical study of convection observed during the winter monsoon experiment using a mesoscale two-dimensional model, *J. Atmos. Sci.*, 1989; **46:** 3077-3107.

[19] Mlawer E.J., Taubman S.J., Brown P.D., Iacono M.J. and Clough S.A., Radiative transfer for inhomogeneous atmospheres: RRTM, a validated correlated-k model for the longwave, *J. Geophys. Res-Atmos.*, 1997, **102:** 16663-16682.

[20] Hong S.Y. and Pan H.L., Nonlocal boundary layer vertical diffusion in a medium-range forecast model, *Mon. Weather, Rev.*, 1996; **124:** 2322-2339.

[21] Chen F. and Dudhia J., Coupling an advanced land surface-hydrology model with the Penn State-NCAR MM5 modeling system. Part I: Model implementation and sensitivity, *Mon. Weather, Rev.*, 2001; **129:** 569-585.

[22] Janjic Z.I., Comments on Development and evaluation of a convection scheme for use in climate models, *J. Atmos. Sci.*, 2000; **57:** 3686-3686.

[23] Grell G.A. and Devenyi D., A generalized approach to parameterizing convection combining ensemble and data assimilation techniques, *Geophys. Res. Lett.*, 2002: 29.

[24] Kain J.S., The Kain-Fritsch convective parameterization: An update, *J. Appl. Meteorol.*, 2004; **43:** 170-181.

[25] Kalnay E., Kanamitsu M., Kistler R., Collins W., Deaven D., Gandin L., Iredell M., Saha S., White G., Woollen J., Zhu Y., Chelliah M., Ebisuzaki W., Higgins W., Janowiak J., Mo K.C., Ropelewski C., Wang J., Leetmaa A., Reynolds R., Jenne R. and Joseph D., The NCEP/NCAR 40-year reanalysis project, *B. Am. Meteorol. Soc.*, 1996; **77:** 437-471.

[26] Mass C.F., Albright M., Ovens D., Steed R., MacIver M., Grimit E., Eckel T., Lamb B., Vaughan J., Westrick K., Storck P., Colman B., Hill C., Maykut N., Gilroy M., Ferguson S.A., Yetter J., Sierchio J.M., Bowman C., Stender R., Wilson R. and Brown W., Regional environmental prediction over the Pacific Northwest, *B. Am. Meteorol. Soc.*, 2003; **84:** 1353-+.

[27] Salathe E.P., Steed R., Mass C.F. and Zahn P.H., A high-resolution climate model for the US Pacific northwest: Mesoscale feedbacks and local responses to climate change, *J. Climate*, 2008; **21:** 5708-5726.

[28] Stauffer D.R. and Seaman N.L., Use of four-dimensional data assimilation in a limited-area mesoscale model, Part I: Experiments with synoptic-scale data, *Mon. Wea. Rev.*, 1990; **118:** 1250-1277.

[29] Stauffer D.R., Seaman N.L. and Binkowski F.S., Use of four-dimensional data assimilation in a limited-area mesoscale model. Part II: Effects of data assimilation within the planetary boundary layer, *Mon. Wea. Rev.*, 1991; **119:** 734-754.

[30] New M., Lister D., Hulme M. and Makin I., A high-resolution data set of surface climate over global land areas, *Clim. Res.*, 2002; **21:** 1-25.

[31] Mitchell T.D. and Jones P.D., An improved method of constructing a database of monthly climate observations and associated high-resolution grids, *Int. J. Climatol.*, 2005; **25:** 693-712.